Viral gene drive spread during herpes simplex virus 1 infection in mice

Authors

Marius Walter[1,2]*, Rebeccah Riley[2], Anoria K Haick[1], Paola A Massa[1], Daniel E Strongin[3], Lindsay M Klouser[1], Michelle A Loprieno[1], Lawrence Stensland[3], Tracy K Santo[3], Matthew P Taylor[4], Keith R Jerome[1,3]*, Eric Verdin[2]*.

[1] Vaccine and Infectious Disease Division, Fred Hutch Cancer Center, Seattle, WA, United States.
[2] Buck Institute for Research on Aging, Novato, CA, United States.
[3] Department of Laboratory Medicine and Pathology, University of Washington, Seattle, WA, United States.
[4] Department of Microbiology & Cell Biology, Montana State University, Bozeman, MT, United States.

*Correspondence to mwalter2@fredhutch.org, everdin@buckinstitute.org, and kjerome@fredhutch.org

Abstract

Gene drives are genetic modifications designed to propagate efficiently through a population. Most applications rely on homologous recombination during sexual reproduction in diploid organisms such as insects, but we recently developed a gene drive in herpesviruses that relies on the co-infection of cells by wild-type and engineered viruses. Here, we designed a viral gene drive against human herpes simplex virus 1 (HSV-1) and showed that it propagated efficiently *in vitro* and during HSV-1 infection in mice. We observed high levels of gene drive-mediated recombination in neuronal tissues as the infection progressed from the site of inoculation to the peripheral and central nervous systems. These findings indicated that HSV-1 achieves high rates of co-infection and recombination during an infection, a phenomenon that is currently underappreciated. Together, this study shows that a viral gene drive can spread *in vivo* during HSV-1 infection, paving the way toward therapeutic applications.

Introduction

Herpesviruses are ubiquitous pathogens that establish lifelong infections and persistently infect most of the human population. Their large dsDNA genomes (100–200 kb) replicate in the nucleus and encode hundreds of genes. After primary infection, herpesviruses enter latency and occasionally reactivate, causing recurrent disease. Herpes simplex viruses (HSV) 1 and 2 first infect mucosal surfaces before spreading to the nervous system via axons. They remain latent in neurons in sensory and autonomic ganglia and reactivation causes lesions in the facial or genital area, which can be highly painful and stigmatizing. HSV-1 and 2 lack vaccines or curative treatments and new therapeutic strategies for HSV diseases are critically needed.

During an infection, cells are often co-infected by several virions and therapeutic approaches that rely on viral co-infection have great potential. These viral interference strategies rely on defective viral particles that interfere with the replication of wild-type viruses after co-infection, thus reducing viral levels (1). Most viral interference approaches have focused on RNA viruses such as SARS-CoV-2, RSV, Influenza, Zika, Chikungunya, or HIV (2–7). We recently developed a system of viral interference against herpesviruses, using a technique of genetic engineering known as a gene drive (8, 9). Gene drives are genetic modifications designed to spread efficiently through a population (10). They usually rely on CRISPR-mediated homologous recombination during sexual reproduction to efficiently spread a transgene in a population, and most applications have been developed in insects to eradicate diseases such as malaria. By contrast, the viral gene drive that we invented spread by the co-infection of cells with wild-type and engineered viruses (Fig. 1A). Specifically, upon co-infection with a gene drive virus expressing CRISPR-Cas9, the wild-type genome is cut and repaired by homologous recombination, producing new recombinant gene drive viruses that progressively replace the wild-type population. In a proof-of-concept with human cytomegalovirus (hCMV), we previously showed that a viral gene drive propagated efficiently *in vitro* in a population of unmodified viruses (8, 9). Importantly, an attenuated gene drive virus could spread efficiently until the wild-type population had been eliminated, ultimately reducing viral levels. This uncovered a new way to engineer herpesviruses for research or therapeutic purposes. Building on our work, a very recent study followed our approach and showed that a viral gene drive could be designed with HSV-1 and spread *in vitro* (11).

The spread of a viral gene drive relies on cellular co-infection events, which occur at a high frequency in cell culture experiments. While numerical simulations suggest that a viral gene drive could still spread with low co-infection rates (8), the frequency of co-infection events during animal or human infections is poorly characterized. In mice, high levels of recombination are observed during herpes simplex encephalitis (12, 13), and attenuated viruses –which individually are harmless– can complement each other and cause severe disease (14, 15).

Moreover, HSV strains circulating in humans exhibit evidence of extensive recombination (16–19). These indirect observations suggest that cells are often co-infected by several virions during infection with HSV-1 or related herpesviruses. However, whether a viral gene drive could propagate *in vivo* remains unknown.

In the present study, we tested if a viral gene drive could spread in animal models of herpesvirus infection. HSV-1 is an important human pathogen with established infection protocols in mice, and we developed a gene drive that targeted a neutral region in the HSV-1 genome. This design was not intended to impact viral fitness or limit viral spread, but to investigate the potential of the technology *in vivo*. Our results show that a gene drive could spread efficiently during HSV-1 infection in mice, in particular in neuronal tissues.

Results

Design of a gene drive against HSV-1

We aimed to build a gene drive that would not affect viral infectivity and could spread efficiently into the wild-type population. We designed a gene drive targeting an intergenic sequence between the UL37 and UL38 genes, a region known to tolerate the insertion of transgenes with little or no impact on viral replication *in vitro* and *in vivo* (20, 21). We cloned a donor plasmid containing homology arms, *Cas9* (from Streptococcus pyogenes) under a CBH promoter, an *mCherry* fluorescent reporter under a CMV promoter, and a U6-driven gRNA targeting the UL37-UL38 region (Fig. 1B). Vero cells were co-transfected with purified HSV-1 viral DNA and the gene drive donor plasmid, and mCherry-expressing viruses created by homologous recombination were isolated by three rounds of plaque purification until a pure population of gene drive virus (GD) was obtained. To follow recombination events between viral genomes, the gene drive virus also carried a cyan fluorescent reporter (CFP) inserted into another neutral region between the *US1* and *US2* viral genes (12, 22) (Fig. 1C). In addition, we similarly built two control viruses with non-functional CRISPR systems, one with a non-specific gRNA (GD-ns) that did not target HSV-1, and one with *Cas9* deleted (GD-ΔCas9). Finally, to be used as a wild-type virus with an unmodified *UL37-UL38* region, we generated a virus expressing a yellow fluorescent reporter (YFP) from the same *US1-US2* region, referred hereafter as HSV1-WT or simply WT (Fig. 1C). All the viruses described here originated from the highly neurovirulent HSV-1 strain 17+.

Recombination between gene drive and wild-type genomes can result in four different genome configurations expressing the different fluorescent reporters, which can be followed by plaque assay (Fig. 1D and 1E). In highly susceptible cell lines such as Vero cells, viral plaques originate from single virions, which allows reconstituting the recombination history of individual viral genomes. Plaques expressing YFP only, or CFP and mCherry together, represent the original WT

and gene drive viruses, respectively, while plaques expressing CFP only, or YFP and mCherry together, represent recombination products that exchanged the gene drive cassette.

Gene drive spread in cell culture

First, we tested if our gene drive could spread *in vitro* and conducted co-infection experiments in cell culture. Some cell lines, and in particular Vero cells or other epithelial cells, efficiently restrict co-infection by a mechanism known as superinfection exclusion (23, 24). However, we found that mouse neuronal N2a cells could sustain high levels of co-infection (Supplementary Fig. S1). Thus, co-infection experiments were conducted in N2a cells, while plaque assays were performed in Vero cells. Importantly, the WT, GD, GD-ns and GD-ΔCas9 viruses individually replicated with similar dynamics in N2a cells, showing that insertion of the gene drive cassette in the *UL37-UL38* region did not affect infectivity *in vitro,* as expected (Fig. 2A).

To test if the gene drive could efficiently spread in the viral population, N2a cells were co-infected with WT+GD, WT+GD-ns, or WT+GD-ΔCas9. Cells were infected with an initial proportion of gene drive virus of 20% at a combined MOI of 1 (Fig. 2B, 2D and 2E). Titers and the proportion of viruses expressing the different fluorescent markers were measured by plaque assay for 3 days. The proportion of viruses expressing mCherry, which represent gene drive viruses, increased from 20% to 85% when cells were co-infected with WT+GD (Fig. 2D). Importantly, YFP-only viruses disappeared and were replaced by recombinant viruses expressing YFP and mCherry, representing 45% of the final population (Fig. 2E). This indicated that the WT population had been converted to new recombinant gene drive viruses, as anticipated. The proportion of viruses expressing CFP and mCherry, which represent the original gene drive virus, increased slightly from 20% to 40% (Fig. 2E). By contrast, in the control experiments with GD-ns and GD-ΔCas9, the proportion of mCherry-expressing viruses did not change and remained close to its initial value around 20% (Fig. 2D). In these control experiments, around 10% of viruses expressed YFP and mCherry at day 3, but this population of recombinant viruses was mirrored by viruses that had lost mCherry and expressed CFP only (Fig. 2E). These represented viruses that had exchanged their YFP and CFP regions in a nonspecific manner. Importantly, CFP-only viruses were not observed after co-infection with WT+GD, highlighting that the efficient incorporation of the gene drive cassette into unmodified genomes is a unilateral and targeted process requiring both Cas9 and a specific gRNA.

To confirm these observations, we repeated these co-infection experiments with an initial proportion of gene drive virus of 40% (Fig. 2C, 2F, and 2G). With this higher starting point, the gene drive achieved almost complete penetrance and the proportion of mCherry-expressing viruses reached 95% after 3 days, with the population of wild-type viruses expressing YFP-only being converted to recombinant gene drive viruses expressing YFP and mCherry. As observed above, In the WT+GD-ns and WT+GD-ΔCas9 control experiments, the proportion of mCherry-expressing viruses remained constant at around 40%, and around 15% of YFP+mCherry

and CFP-only viruses symmetrically appeared by nonspecific recombination. This further showed that a gene drive could spread efficiently in the wild-type population and that the drive was mediated by a functional CRISPR system.

Together, these results indicated that a gene drive could be designed against HSV-1 and spread efficiently *in vitro.* Importantly, both during single and co-infections, viral titers followed similar dynamics (Fig. 2A-2C), and the proportion of viruses expressing CFP remained constant, indicating that the rapid increase of recombinant viruses expressing mCherry and YFP cannot be explained by a higher fitness of the GD virus. These results corroborated the results of a recent study (11) and expanded on our previous work with hCMV, showing that a viral gene drive could be designed in a second, unrelated, herpesvirus. In our hCMV study, we characterized individual genomes and conducted long-read sequencing of recombinant viruses (8). These analyses demonstrated that the gene drive sequence was specifically transferred from one viral strain to the other, with plaque assays and sequencing analyses delivering identical conclusions. By analogy, the results obtained here with HSV-1 indicated that CRISPR-mediated homologous recombination directed the efficient spread of the gene drive in the wild-type population.

Gene drive spread during herpes encephalitis

Next, we tested if the gene drive could spread during acute HSV-1 infection in mice. Previous studies using similar fluorescent reporters showed that HSV-1 naturally reaches high levels of recombination in the mouse brain during herpes simplex encephalitis (12). Thus, we hypothesized that a gene drive could spread efficiently in this context. We used a well-established infection model, where HSV-1 is inoculated intravitreally in the eye and infects the retina and other ocular tissues before propagating to the nervous system via cranial nerves (Fig. 3A). Specifically, HSV-1 either travels directly to the brain via the optic and oculomotor nerves (cranial nerve CN II and III, respectively), or indirectly by first infecting ganglionic neurons of the peripheral nervous system. In particular, HSV-1 travels to the trigeminal ganglia (TG) via the trigeminal nerve (CN V) before reaching the brain stem. In the following experiments, a total of 10^6 plaque forming units (PFU) were inoculated intravitreally in the left eye, and tissues were collected, dissociated, and analyzed by plaque assay after four days. Five to eight-week-old male and female Balb/c mice were used and we did not observe any differences between the sexes. Importantly, individual infections with WT, GD and GD-ns reached similar titers in the eye, the TG and the brain, showing that the gene drive cassette in the *UL37-UL38* region did not impact infectivity *in vivo* (Fig. 3B).

To test if the gene drive could efficiently spread *in vivo*, mice were inoculated intravitreally with WT only, WT+GD, or WT+GD-ns, with an initial proportion of gene drive virus of 15% (Fig. 3C-3E). Titers in the eye, TG and brain after four days were indistinguishable between the different conditions, showing that the gene drive did not perturb the overall dynamics of infection (Fig. 3C). The population of gene drive viruses expressing mCherry increased from 15% to 30% in the

eye, to 60% in the TG, and 70% in the brain, respectively. We observed a high variation between replicates, with the percentage of gene drive viruses in the brain ranging from 50% to 90%, with a median of 77%. Furthermore, and as observed *in vitro,* wild-type viruses expressing YFP-only were converted to recombinant gene drive viruses expressing YFP and mCherry, representing 40% of the final population. The proportion of original gene drive virus viruses expressing CFP and mCherry increased slightly, from 15% to 20% in the TG, and to 30% in the brain, respectively (Fig. 3C). Critically, in the control experiment with GD-ns, the proportion of gene drive viruses did not change and remained close to its initial value around 15% in all tissues, with a similar proportion of YFP+mCherry and CFP-only viruses appearing by nonspecific recombination. Altogether, this important result shows that the gene drive efficiently spread in the viral population as the infection progressed to the brain, with recombinant gene drive viruses increasing from 15% to 70% in four days.

Gene drive propagation relies on efficient homologous recombination after CRISPR cleavage, but DNA double-strand breaks can also be repaired by non-homologous end joining (NHEJ), resulting in small insertions and deletions that render viruses resistant to the drive (9). After PCR and Sanger sequencing of infectious viruses isolated from the brain, we found that 20% of the remaining target sites had been mutated by NHEJ (Fig. 3F). Since the gene drive represented 70% of viruses at this point, this result suggested that drive-resistant viruses represented around 6% of the total viral population. This indicated that the drive did not achieve full penetrance after four days, and confirmed the observation made with hCMV that repair by NHEJ is infrequent compared to homologous recombination during gene drive spread (8, 9).

We next tested if our gene drive could spread in another infection model, where HSV-1 is inoculated in the hind leg footpad. In this model, HSV-1 travels to the spinal cord via the sciatic nerve, and finally to the brain. 10^6 pfu of WT, WT+GD or WT+GD-ns were inoculated in the right hind footpad, with an initial proportion of gene drive virus of 15%. Tissues were collected five to seven days later and analyzed by plaque assay (Fig. 3G-I). Around half the mice did not show any symptoms of infection and had no detectable titers in the spinal cord and the brain, while others developed severe neurological symptoms with very high titers (Fig. 3G). In animals with detectable viral levels, the proportion of gene drive viruses increased from 15% to 60% in the brain, with a range between 30% and 80%, and reached 50% in the spinal cord (Fig. 3H). Once again, wild-type viruses expressing YFP-only had been converted to recombinant gene drive viruses expressing YFP and mCherry, while the population of viruses expressing CFP and mCherry remained constant (Fig. 3G). Only one control animal infected with WT+GD-ns developed a detectable infection, with mCherry-expressing viruses reaching 35% in the spinal cord. These results confirmed that a gene drive could spread in a second route of HSV-1 infection.

Altogether, these findings showed that a gene drive could propagate efficiently *in vivo* during acute HSV-1 infection in mice, and that the drive was mediated by a functional CRISPR system.

High heterogeneity during gene drive spread in the brain

HSV-1 travels to the brain via different neuronal pathways, and we hypothesized that following gene drive propagation in different regions of the brain could bring novel insight into the dynamic of HSV-1 infection and recombination. After intravitreal inoculation, HSV-1 infects retinal neurons and travels via the optic nerve (CN II) to the hypothalamus and the thalamus, both part of the interbrain–, before reaching the cortex through visual pathways. Secondary branches of the optic nerve also connect to the midbrain –the upper part of the brain stem. After infecting other ocular tissues, HSV-1 also reaches the midbrain via the oculomotor nerve (CN III), first connecting to the ciliary ganglion located behind the eye. Finally, HSV-1 travels via the trigeminal nerve (CN V) to the trigeminal ganglia and then to the medulla –the lower part of the brain stem (Fig. 4A).

To investigate tissue-specific differences in gene drive propagation, Balb/c mice were inoculated intravitreally with 10^6 PFU of WT+GD, with an initial proportion of gene drive virus of 15%. Titers and gene drive-mediated recombination were measured by plaque assay in the eye, TG, brain stem, interbrain, cortex and cerebellum for four days (Fig. 4). Titers increased progressively throughout the brain, first reaching the interbrain and brain stem after 2 days and then spreading to the cortex and cerebellum (Fig. 4B and summary heatmap in Fig. 4E, upper panel). As described above, the proportion of gene drive viruses remained low in the eye, and reached around 60% in the TG (Fig. 4C-4E). Interestingly, gene drive levels varied greatly between the different brain regions. The gene drive reached 80% in the brain stem after only two days, and progressively increased to 65% in the interbrain and cerebellum, with a penetrance of up to 90% in some animals. By contrast, gene drive levels remained low in the cortex, at 25% on average. As observed above, in the TG, brain stem and interbrain –but not in the eye and cortex, viruses expressing YFP-only had been converted to recombinant gene drive viruses expressing YFP and mCherry (Fig. 4D). Together, this showed that gene drive spread in the brain is highly heterogeneous, with almost complete penetrance in some regions and barely any in adjacent ones.

Discussion

In this manuscript, we designed a gene drive against HSV-1 and showed that it could spread efficiently both *in vitro* and *in vitro.* Our *in vitro* results recapitulated our previous work with hCMV and aligned with the findings of a recent preprint (8, 11). Together, this showed that a gene drive could be designed in a second herpesvirus with very different infection dynamics.

This suggests that viral gene drives could be designed in a wide variety of herpesviruses, which significantly expands the potential of the technology.

The spread of a viral gene drive relies on the co-infection of cells by wild-type and engineered viruses. High co-infection levels can easily be achieved in cell culture, either by using cell lines naturally susceptible to co-infection such as N2a cells, or by infecting cells at a high MOI to bypass restriction mechanisms (11). However, whether co-infection events occur at high frequency *in vivo* was unknown. Here, we showed that a gene drive could spread efficiently during herpes encephalitis in mice, with the level of gene drive-mediated recombination increasing from 15% to 80% in some brain regions after only four days. These findings indicated that HSV-1 achieves high rates of co-infection and recombination during viral spread. This phenomenon is underappreciated and will be the subject of further studies.

Interestingly, we observed a high heterogeneity in gene drive levels in different brain regions (Fig. 4). This heterogeneity gives an interesting insight into the dynamic of HSV-1 infection. Gene drive propagation relies on cellular co-infection and one intuitive hypothesis is that higher viral levels would increase the probability that cells are co-infected by several virions, and, thus, that recombination levels should positively correlate with viral titers. However, no correlation between titers and recombination was observed (Supplementary Fig. 2). For example, HSV-1 levels were the highest in the eye, but gene drive levels remained the lowest in this organ. Similarly, HSV-1 reached similar titers in the brain stem, interbrain and cortex, but almost no recombination occurred in the cortex while high levels were observed in the brain stem and interbrain (Fig. 4D). This shows that recombination does not simply correlate with viral titers, as could be expected, but is likely explained by other tissue-specific cellular or viral mechanisms.

Importantly, this research could pave the way for therapeutic applications in the future. This manuscript presented a proof-of-concept that a gene drive can spread *in vivo*. This represents an important milestone toward designing therapeutical gene drives. Our future work will focus on designing gene drives that can limit infectivity and reduce disease severity, either during an acute infection, like here, or in the context of a latent infection. As a final note, the development of gene drives in mosquitoes and other insects has generated important ecological and biosafety concerns (25). Our approach followed the guidelines established by the NIH and the National Academy of Science (26, 27). In the future, the risks and benefits of viral gene drives will need to be properly addressed and discussed with the scientific community.

Materials and Methods

Cells and viruses

Green monkey epithelial Vero cells and murine neuroblastoma N2a cells were obtained from the ATTC and cultured in DMEM (Corning, Corning, NY, USA) supplemented with 10% FBS (Sigma-Aldrich, St-Louis, MO, USA). Cells were maintained at 37 °C in a 5% CO_2 humidified incubator and frequently tested negative for mycoplasma contamination.

Unmodified HSV-1 strain 17+ and HSV-1-CFP expressing Cyan fluorescent protein mTurquoise2 from the US1/2 locus were provided by Matthew Taylor (University of Montana, USA). Viruses generated for this study were made by modifying HSV-1 and HSV-1-CFP, as described below. To prepare viral stocks for cell culture experiments, Vero cells in 15 cm dishes were infected for one hour at MOI=0.01, and kept in culture for 48 hours or until 100% cytopathic effect was observed. Cells and supernatant were scraped out of the plate, sonicated three times at maximum power with a probe sonicator, and debris pelleted away by centrifugation (2000 rpm, 10 minutes, 4 °C). Media containing viruses was collected in single-use aliquots and titers assessed by plaque assay.

For high-titer and high-purity viral stocks used for animal experiments, Vero cells in 15 cm dishes were infected for one hour at MOI=0.01, and kept in culture for 48 hours or until 100% cytopathic effect was observed. Supernatants and cells were collected, and cells pelleted by centrifugation (2000 rpm, 5 minutes, 4 °C). Supernatants were collected in clean tubes and reserved for later. Cell pellets were resuspended in a small volume and cell-bound virions were released by two cycles of freeze-thaw in dry ice. Debris were pelleted again and discarded, while the supernatant containing released virions was combined with the initial supernatant. Virions were then pelleted by ultracentrifugation (22 krpm, 90 min, 4 °C, Beckman-Coulter rotor SW28) on a 5-mL cushion of 30% sucrose. Supernatants were discarded, and virions were resuspended in PBS containing 2% BSA. Single-use aliquots were prepared and titers were assessed by plaque assay.

Co-infection experiments were performed in 12-well plates by co-infecting N2a cells with HSV-1-WT and gene drive viruses for 1 h, with a total MOI of 1, before replacing inoculum with 1mL of fresh medium. 100uL of supernatant was collected at regular intervals and analyzed by plaque assay.

Cloning and generation of recombinant viruses.

A donor plasmid containing the gene drive cassette against the HSV-1 UL37-38 region (GD and derivatives) was generated by serial modifications of the GD-mCherry donor plasmid generated in our previous study (8). All modifications were carried out by Gibson assembly (NEB, Ipswich, MA, USA), using PCR products from other plasmids or synthesized DNA fragments (GeneArtTM StringTM fragments, ThermoFisher, USA). The final GD donor plasmid included homology arms

for the UL37-38 region, a CBH promoter driving *spCas9* followed by an SV40 polyA terminator, a CMV promoter driving an *mCherry* reporter followed by a betaGlobin polyA signal, and a U6 promoter controlling gRNA expression. The functional GD plasmid carried a gRNA targeting the UL37-38 region (ACGGGATGCCGGGACTTAAG), while the non-specific GD-ns control targeted a sequence not present in HSV-1 (ACATCGCGGTCGCGCGTCGG). GD-ΔCas9 donor construct was subsequently generated by removing SpCas9 by digestion and ligation. A donor construct to insert a CMV-driven Yellow fluorescent protein (YFP) reporter into the US1/US2 locus was built similarly, by replacing *mTurquoise* with *mCitrine2* in a donor plasmid for the US1/US2 region (pGL002, from Matthew Taylor).

To build gene drive viruses and derivatives, 1.5 million Vero cells were co-transfected with linearized donor plasmids and purified HSV-1-CFP viral DNA. Viral DNA was purified from infected cells by HIRT DNA extraction, as described previously (8). Transfection was performed by Nucleofection (Lonza, Basel, Switzerland) and cells were plated in a single 6-well. After 2–4 days, mCherry-expressing viral plaques were isolated and purified by several rounds of serial dilutions and plaque purification. Purity and absence of unmodified viruses were assayed by PCR and Sanger sequencing after DNA extraction (DNeasy kit, Qiagen). HSV1-WT expressing YFP from the US1/US2 region was built similarly by co-transfecting the YFP donor plasmid and HSV-1 strain 17+ purified DNA. Viral stocks were produced as specified above and titered by plaque assay.

Plaque assay

Viral titers and recombination levels were assayed by plaque assay with 10-fold serial dilutions. Confluent Vero cells in 24-well plates were incubated for 1 h with 100uL of inoculum, and overlaid with 1mL of complete media containing 1% methylcellulose, prepared using DMEM powder (Thermo) and Methylcellulose (sigma). After two or three days, fluorescent plaques expressing YFP, CFP and/or mCherry were manually counted using a Nikon Eclipse Ti2 inverted microscope. Every viral plaque was analyzed on both YFP, CFP and red channel. 5–100 plaques were counted per well, and each data point was the average of 3–4 technical replicates (i.e., 3–4 different wells). Images of fluorescent viral plaques were acquired with an EVOS automated microscope and adjusted for contrast and exposure with ImageJ (v2.1.0).

The deconvolution of Sanger sequencing in Fig. 3F was performed using Synthego ICE online tools (https://ice.synthego.com).

Mouse experiments

Male and female Balb/c between five and eight weeks old were used for *in vivo* studies. Mice were maintained at the Buck Institute vivarium. All procedures were performed following federal guidelines and approved by the Buck Institute Institutional Animal Care and Use Committees (IACUC). Mice were infected by intravitreal injection in the left eye, as described previously (28,

29). Briefly, mice will be anesthetized with ketamine/xylazine and laid prone on a sterile pad. The left eye was treated with a thin layer of veterinary ophthalmic ointment and the sclera was exposed using an ophthalmic forceps. The viral inoculum was injected slowly in the intravitreal space, using a 5uL Hamilton syringe and a 30 gauge needle. 2 µl of HSV virus stock containing 10^6 pfu was used. In the days following infection, mice were treated with sustained-release buprenorphine to minimize pain (Ethiqa XR, Fidelis Animal Health, North Brunswick, New Jersey, USA). Animals were humanely euthanized after two to four days. Tissues were collected and snap-freezed in liquid nitrogen.

To release infectious virions, frozen tissues were resuspended in cell culture media and disrupted using a gentle tissue homogenizer (Pellet Pestle, Fisher Scientific, USA). Samples were sonicated three times at maximum power with a probe sonicator, and debris pelleted away by centrifugation (2000 rpm, 10 minutes, 4 °C). Volume was adjusted to a final volume of 1mL, and titers were subsequently measured by plaque assay.

Statistics and reproducibility

Experiments were carried out in multiple replicates and investigators were blinded when performing plaque assays. Statistical analyses were run using GraphPad Prism version 10.1.1 for macOS (GraphPad Software, USA, www.graphpad.com).

Acknowledgments

We thank members of the Verdin and Jerome lab for technical and conceptual help. This study was funded through institutional support from the Buck Institute for Research on Aging and the Fred Hutch Cancer Center.

Author contributions

MW designed the study with input from EV, KRJ and MPT. MW performed all *in vitro* experiments. MW and RR wrote the IACUC protocol at the Buck Institute. MW, RR, AKH, PAA, MAL and DES contributed to mouse husbandry and mouse experiments. LMK, LS and TKS processed samples at the University of Washington Virology Laboratory. MW, MPT, KRJ and EV analyzed the data. MW wrote the manuscript with input from all authors. EV and KRJ supervised and funded the project.

Competing interests

A patent application describing the use of a gene drive in DNA viruses has been filed by the Buck Institute for Research on Aging (Application number 17054760, inventor: M.W.). The authors declare no further competing interests.

References

1. E. J. Tanner, K. A. Kirkegaard, L. S. Weinberger, Exploiting Genetic Interference for Antiviral Therapy. *PLoS Genet.* **12**, e1005986 (2016).

2. S. Chaturvedi, *et al.*, Identification of a therapeutic interfering particle—A single-dose SARS-CoV-2 antiviral intervention with a high barrier to resistance. *Cell* **0** (2021).

3. N. J. Dimmock, E. W. Rainsford, P. D. Scott, A. C. Marriott, Influenza virus protecting RNA: an effective prophylactic and therapeutic antiviral. *J. Virol.* **82**, 8570–8578 (2008).

4. X. Mercado-López, *et al.*, Highly immunostimulatory RNA derived from a Sendai virus defective viral genome. *Vaccine* **31**, 5713–5721 (2013).

5. V. V. Rezelj, *et al.*, Defective viral genomes as therapeutic interfering particles against flavivirus infection in mammalian and mosquito hosts. *Nat. Commun.* **12**, 2290 (2021).

6. L. I. Levi, *et al.*, Defective viral genomes from chikungunya virus are broad-spectrum antivirals and prevent virus dissemination in mosquitoes. *PLoS Pathog.* **17**, e1009110 (2021).

7. E. J. Tanner, *et al.*, Discovery and Engineering of a Therapeutic Interfering Particle (TIP): a combination self-renewing antiviral. *bioRxiv*, 820456 (2019).

8. M. Walter, E. Verdin, Viral gene drive in herpesviruses. *Nat. Commun.* **11**, 4884 (2020).

9. M. Walter, R. Perrone, E. Verdin, Targeting Conserved Sequences Circumvents the Evolution of Resistance in a Viral Gene Drive against Human Cytomegalovirus. *J. Virol.* **95**, e0080221 (2021).

10. K. M. Esvelt, A. L. Smidler, F. Catteruccia, G. M. Church, Concerning RNA-guided gene drives for the alteration of wild populations. *Elife* **3**, e03401 (2014).

11. H. Dai, *et al.*, Viruses that “infect” viruses: Cas12f1 and Cas9 gene drive in HSV1. *bioRxiv*, 2023.12.04.569968 (2023).

12. G. A. Law, A. E. Herr, J. P. Cwick, M. P. Taylor, A New Approach to Assessing HSV-1 Recombination during Intercellular Spread. *Viruses* **10** (2018).

13. J. P. Card, *et al.*, A dual infection pseudorabies virus conditional reporter approach to identify projections to collateralized neurons in complex neural circuits. *PLoS One* **6**, e21141 (2011).

14. R. T. Javier, F. Sedarati, J. G. Stevens, Two avirulent herpes simplex viruses generate lethal recombinants in vivo. *Science* **234**, 746–748 (1986).

15. Y. Nishiyama, H. Kimura, T. Daikoku, Complementary lethal invasion of the central nervous system by nonneuroinvasive herpes simplex virus types 1 and 2. *J. Virol.* **65**, 4520–4524 (1991).

16. R. Bowden, H. Sakaoka, P. Donnelly, R. Ward, High recombination rate in herpes simplex virus type 1 natural populations suggests significant co-infection1. *Infect. Genet. Evol.* **4**, 115–123 (2004).

17. A. M. Casto, *et al.*, Large, Stable, Contemporary Interspecies Recombination Events in Circulating Human Herpes Simplex Viruses. *J. Infect. Dis.* **221**, 1271–1279 (2020).

18. D. M. Koelle, *et al.*, Worldwide circulation of HSV-2 × HSV-1 recombinant strains. *Sci. Rep.* **7**, 44084 (2017).

19. J. Å. Liljeqvist, P. Tunbäck, P. Norberg, Asymptomatically shed recombinant herpes simplex virus type

1 strains detected in saliva. *J. Gen. Virol.* **90**, 559–566 (2009).

20. W. W. Gierasch, *et al.*, Construction and characterization of bacterial artificial chromosomes containing HSV-1 strains 17 and KOS. *J. Virol. Methods* **135**, 197–206 (2006).

21. M. P. Taylor, O. Kobiler, L. W. Enquist, Alphaherpesvirus axon-to-cell spread involves limited virion transmission. *Proc. Natl. Acad. Sci. U. S. A.* **109**, 17046–17051 (2012).

22. T. Morimoto, J. Arii, H. Akashi, Y. Kawaguchi, Identification of multiple sites suitable for insertion of foreign genes in herpes simplex virus genomes. *Microbiol. Immunol.* **53**, 155–161 (2009).

23. A. Criddle, T. Thornburg, I. Kochetkova, M. DePartee, M. P. Taylor, gD-Independent Superinfection Exclusion of Alphaherpesviruses. *J. Virol.* **90**, 4049–4058 (2016).

24. J. P. Cwick, *et al.*, Superinfection Exclusion of Alphaherpesviruses Interferes with Virion Trafficking. *Microbiol Spectr* **10**, e0068422 (2022).

25. D. Brossard, P. Belluck, F. Gould, C. D. Wirz, Promises and perils of gene drives: Navigating the communication of complex, post-normal science. *Proc. Natl. Acad. Sci. U. S. A.* **116**, 7692–7697 (2019).

26. C. Emerson, S. James, K. Littler, F. (fil) Randazzo, Principles for gene drive research. *Science* **358**, 1135–1136 (2017).

27. E. A. M. National Academies of Sciences, *Gene Drives on the Horizon* (National Academies Press, 2016).

28. J. P. Card, M. E. Whealy, A. K. Robbins, R. Y. Moore, L. W. Enquist, Two alpha-herpesvirus strains are transported differentially in the rodent visual system. *Neuron* **6**, 957–969 (1991).

29. J. P. Card, L. W. Enquist, “Use and visualization of neuroanatomical viral transneuronal tracers” in *Visualization Techniques*, Neuromethods., (Humana Press, 2012), pp. 225–268.

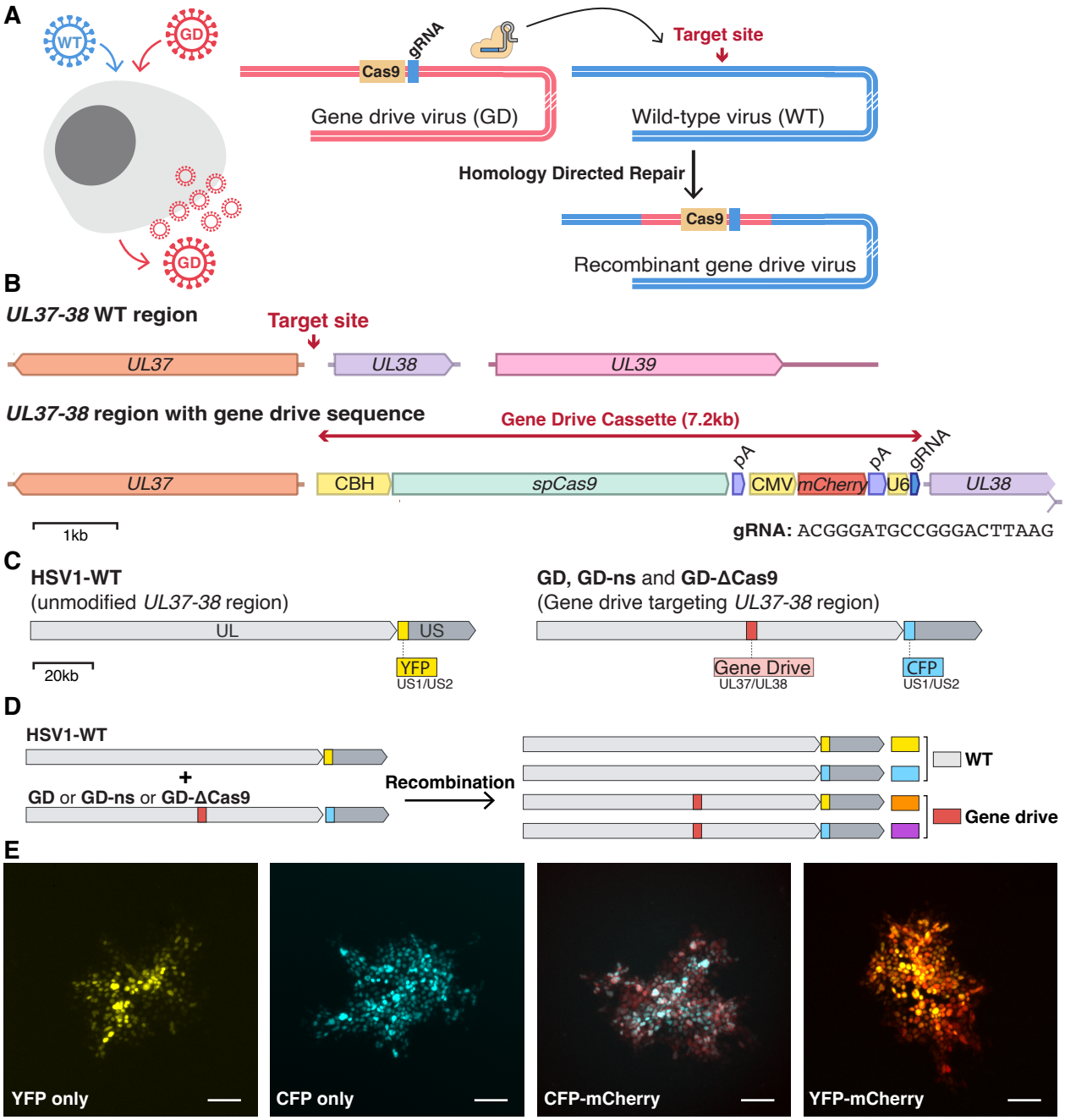

Figure 1: Design of a viral gene drive targeting HSV-1 UL37-38 region.
A. Gene drive viruses carry *Cas9* and a gRNA targeting the same location in a wild-type genome. After co-infection of cells by wild-type (WT) and gene drive (GD) viruses, Cas9 cleaves the wild-type sequence and homology-directed repair –using the gene drive sequence as a repair template– causes the conversion of the wild-type locus into a new gene drive sequence and the formation of new recombinant gene drive viruses. **B**. Modified and unmodified *UL37-38* region. The gene drive cassette was inserted between the *UL37* and *UL38* viral genes, and is composed of *spCas9* under the control of a CBH promoter followed by the SV40 polyA signal, a CMV promoter driving an *mCherry* reporter, followed by the beta-globin polyA signal, and a U6-driven gRNA. **C**. Localizations of the gene drive sequence and YFP/CFP reporters on HSV-1 genomes. GD represents a functional gene drive virus, GD-ns carries a non-specific gRNA, and *Cas9* is deleted in GD-ΔCas9. UL/US: unique long/short genome segments. **D, E**. Potential recombination products and examples of viral plaques after cellular co-infection with HSV1-WT expressing YFP and gene drive viruses expressing mCherry and CFP.

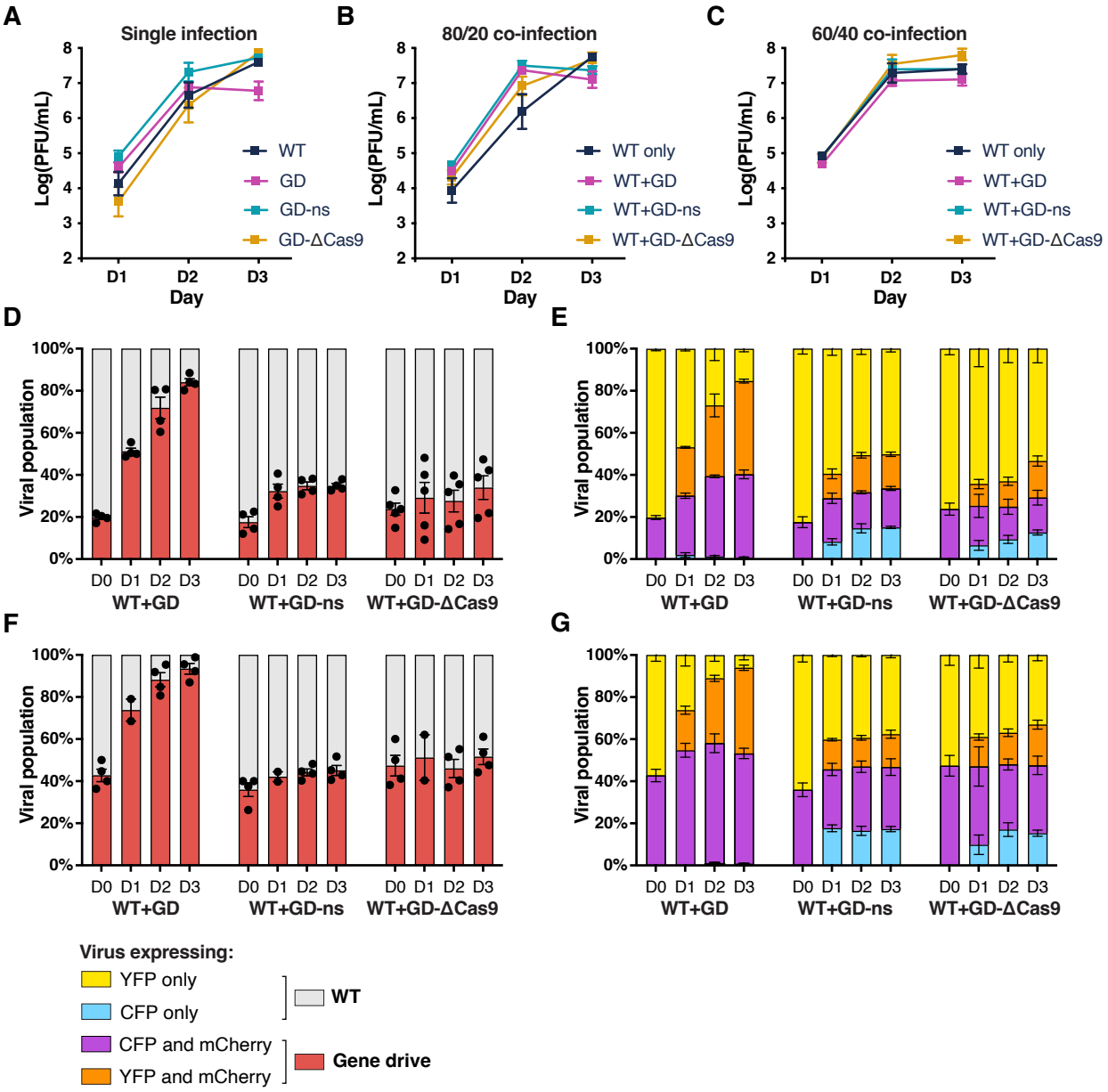

Figure 2: Gene drive spread in cell culture.
A. Viral titers in the supernatant after infection of N2a cells with WT, GD, GD-ns or GD-ΔCas9. Cells were infected with a single virus at MOI=1. n=4. **B, C**. Viral titers in the supernatant after co-infection of N2a cells with WT+GD, WT+GD-ns or WT+GD-ΔCas9, with a starting proportion of gene drive virus of 20% (B) or 40% (C). MOI=1, n=4. **D-G**. Evolution of the viral population after co-infection with WT+GD, WT+GD-ns or WT+GD-ΔCas9, with a starting proportion of gene drive virus of 20% (D, E) or 40% (F, G). Panels D and F shows the proportion of viruses expressing mCherry, representing gene drive virus. Panels E and G shows the proportion of viruses expressing the different fluorophore combinations. Viral titers are expressed in log-transformed PFU (plaque-forming unit) per mL of supernatant. Error bars represent standard error of the mean (SEM) between biological replicates. n=4.

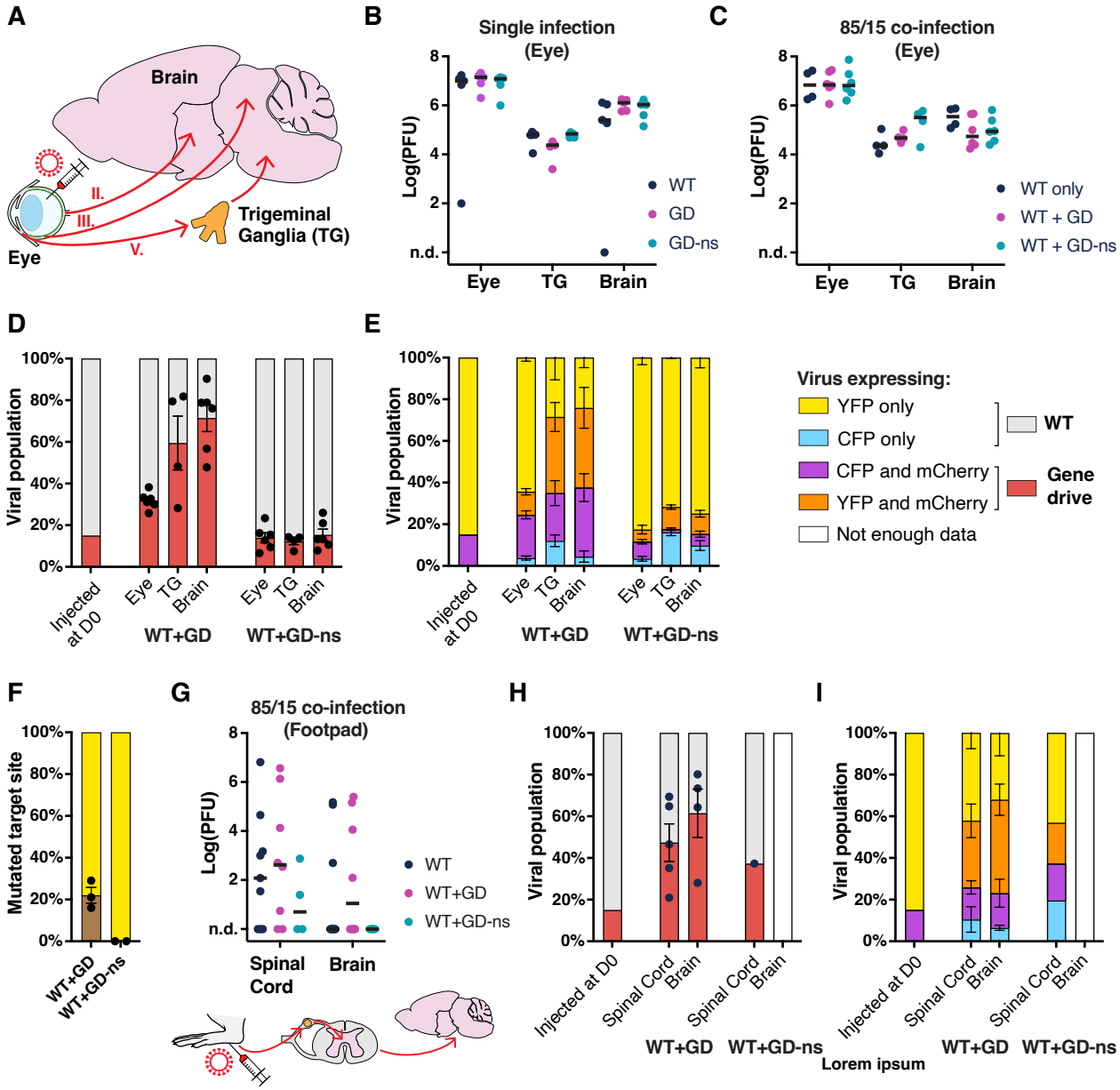

Figure 3: Gene drive spread during herpes simplex encephalitis

A. Infection routes along optic, oculomotor and trigeminal nerves (cranial nerves II, III and V, respectively) following ocular inoculation of HSV-1. Male and female Balb/c mice were infected with 10^6 PFU in the left eye. **B, C**. Viral titers after four days in the eye, TG and whole brain after (B) infection with a single virus, n=5, or (C) with a starting proportion of gene drive virus of 15%. n=6. **D, E**. Viral population in the eye, TG and whole brain after co-infection with WT+GD or WT+GD-ns, after four days. n=6. **F**. Proportion of viral genomes with a mutated target site in the brain after four days. **G**. Viral titers in the spinal cord and brain after inoculation of WT, WT+GD, or WT+GD-ns in the right hind leg footpad, after 5-7 days. n=8 for WT and WT+GD, n=4 for WT+GD-ns. **H, I**. Viral population in the spinal cord and whole brain after co-infection with WT+GD or WT+GD-ns, after 5-7 days. n=5 for WT+GD, n=1 for WT+GD-ns.
Viral titers are expressed in log-transformed PFU. Black lines indicate the median. n.d.: non-detected. Panels D, E, F, H and I show the average and SEM between biological replicates.

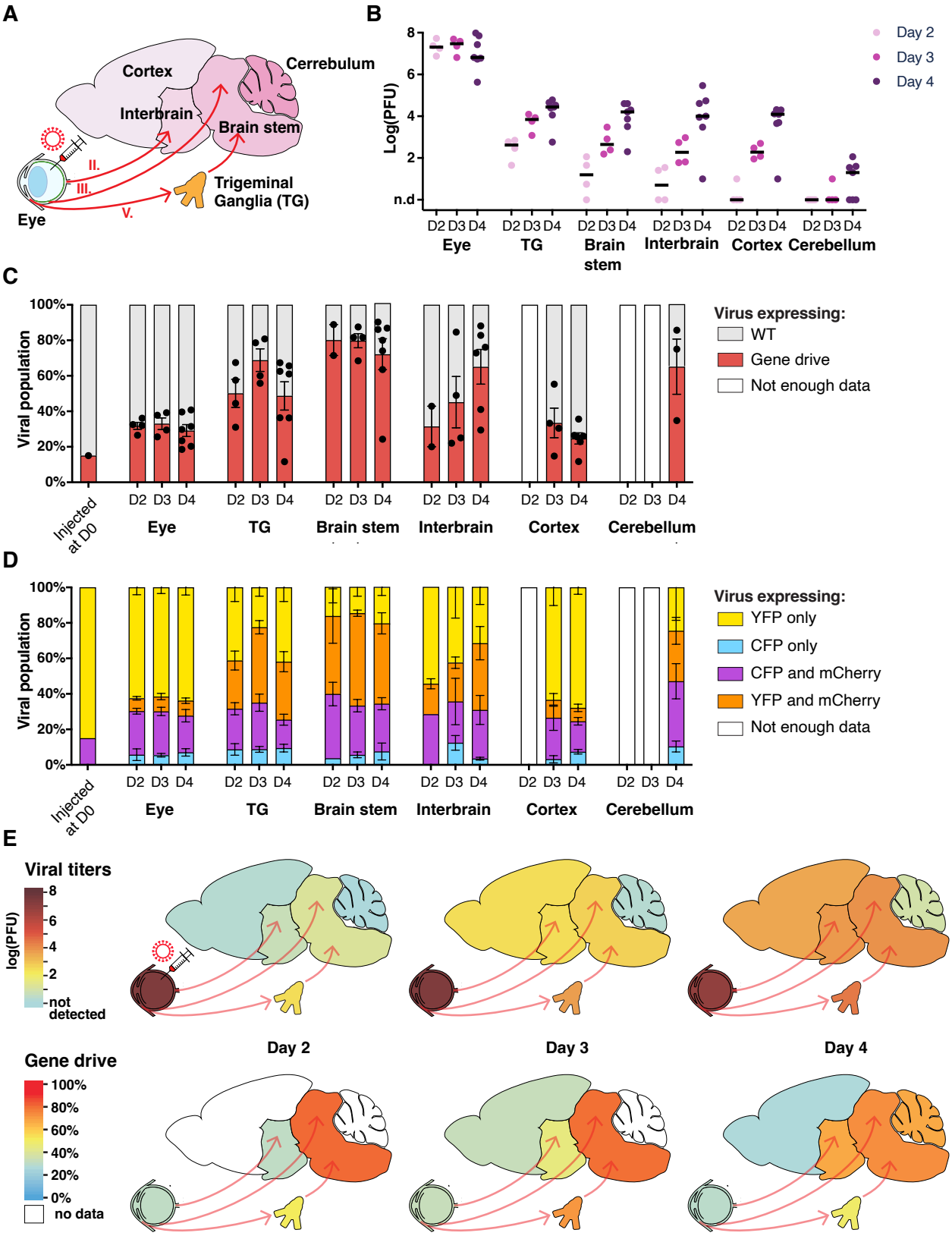

Figure 4: High heterogeneity between brain regions during gene drive spread
A. Infection routes following ocular inoculation of HSV-1. Male and female Balb/c mice were co-infected with 10^6 PFU of WT+GD in the left eye, with a starting proportion of gene drive virus of 15%. **B**. Viral titers over time. **C, D**. Proportion of viruses over time. **E**. Heatmap summarizing panels B and C. Viral titers are expressed in log-transformed PFU. Black lines indicate the median. Panels C and D show the average and SEM between biological replicates. n=4 for day 2 and 3, n=6 for day 4. n.d.: non-detected.

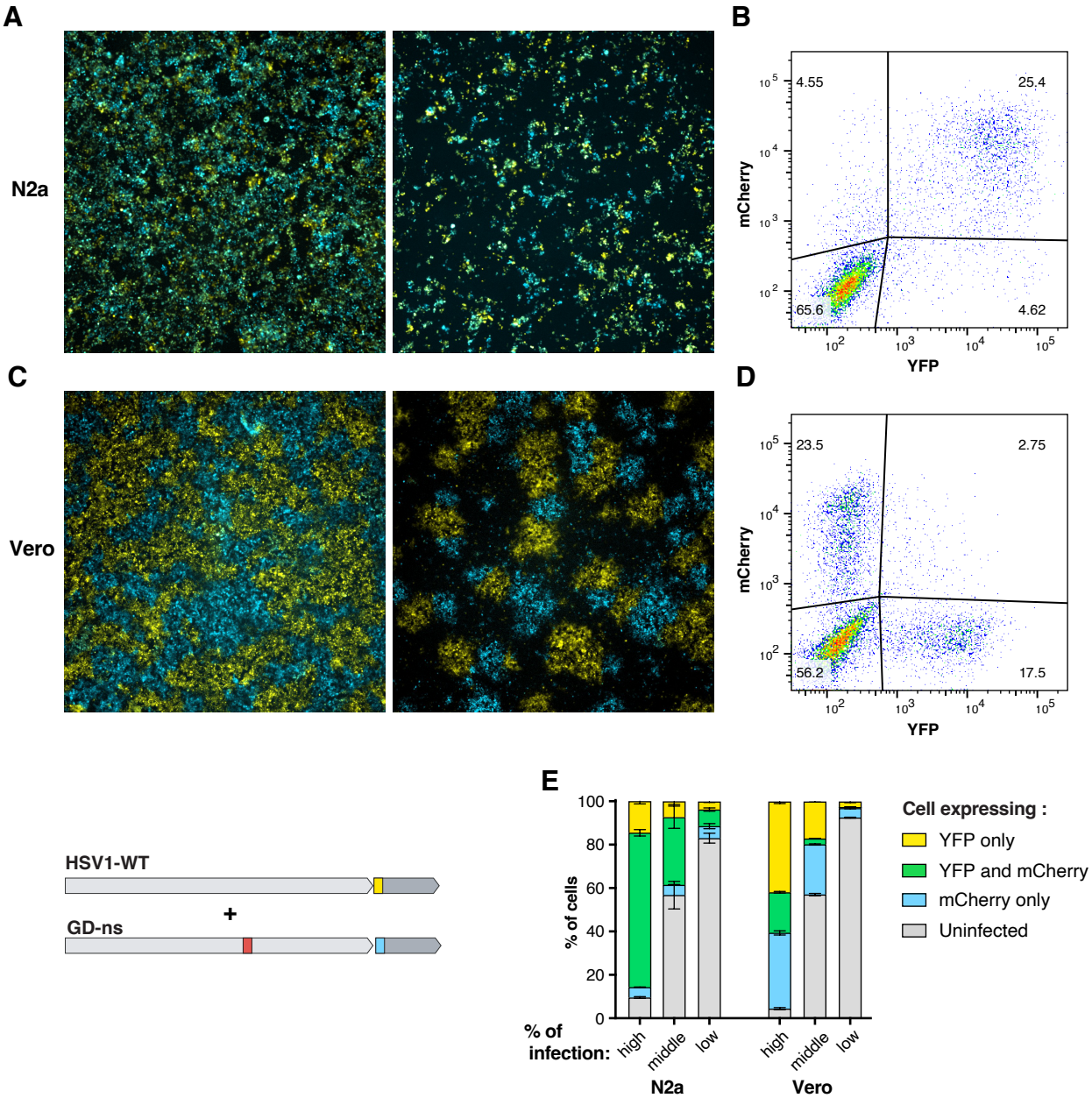

Supplementary Figure S1. N2a cells sustain high levels of co-infection.
N2a and Vero cells were coinfected with WT virus expressing YFP and GD-ns virus expressing CFP and mCherry, at low MOI (from 0.1 to 0.001). Two days later, the proportion of infected and co-infected cells was analyzed by microscopy (A, C) or flow cytometry (B, D and E). At both high, middle, or low total infection rates, N2a cells showed a high level of co-infection, while Vero cells had very little co-infection. In panel E, data show mean and SEM between 6 (high co-infection rate) or 3 (middle and low infection rates) biological replicates. High, middle, and low infection rates indicate that around 90%, 40%, or 10% of all cells are infected, respectively.

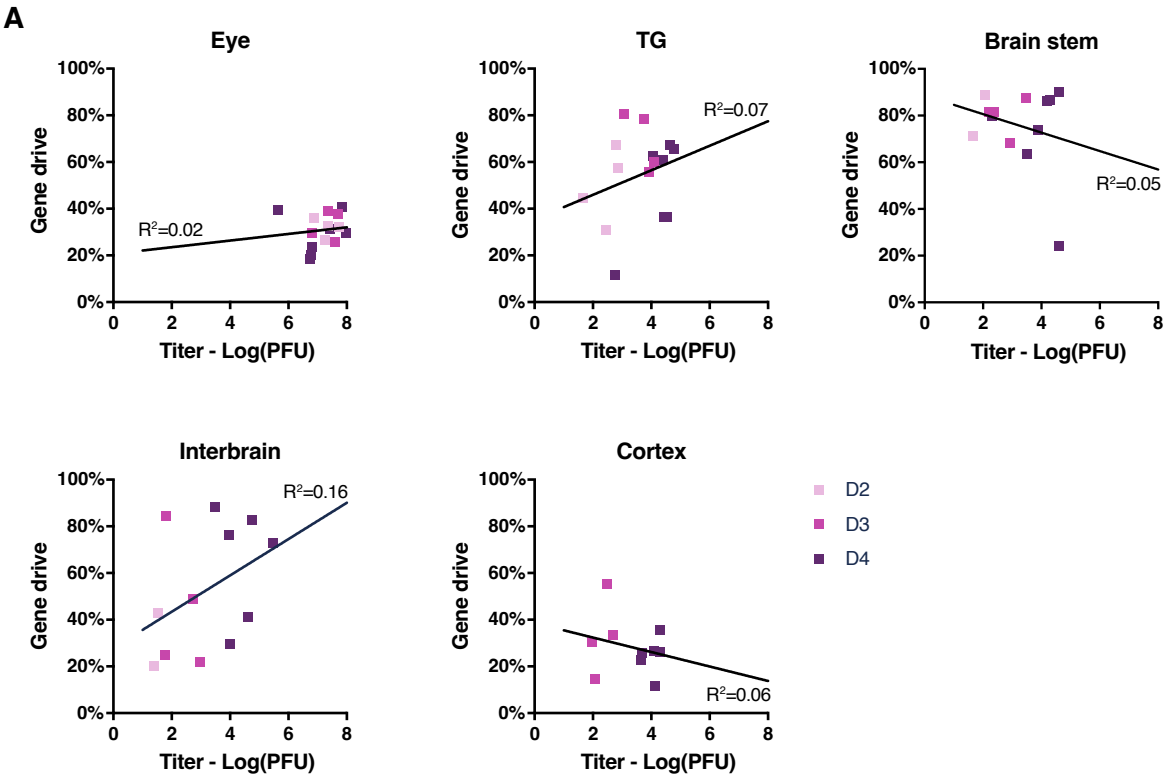

Supplementary Figure S2. No correlation between viral titers and gene drive-mediated recombination.
No correlation was observed after least square linear regression between viral titers and the level of gene drive-mediated recombinants in the different brain regions. R^2 indicate the goodness of fit. .